

PACS numbers: 87.57.–s; 87.19.U–; 42.30.Ms
DOI: 10.1070/QE2012v042n06ABEH014887

Laser speckle-imaging of blood microcirculation in the brain cortex of laboratory rats in stress

M.A. Vilensky, O.V. Semyachkina-Glushkovskaya, P.A. Timoshina, Ya.V. Kuznetsova, I.A. Semyachkin-Glushkovskii, D.N. Agafonov, V.V. Tuchin

Abstract. **The results of experimental approbation of the method of laser full-field speckle-imaging for monitoring the changes in blood microcirculation state of the brain cortex of laboratory rats under the conditions of developing stroke and administration of vasodilating and vasoconstrictive agents are presented. The studies aimed at the choice of the optimal conditions of speckle-image formation and recording were performed and the software implementing an adaptive algorithm for processing the data of measurements was created. The transfer of laser radiation to the probed region of the biotissue was implemented by means of a silica-polymer optical fibre. The problems and prospects of speckle-imaging of cerebral microcirculation of blood in laboratory and clinical conditions are discussed.**

Keywords: *laser speckles, full-field method, contrast of speckle-images, adaptive algorithm, microcirculation, cerebral blood flow.*

1. Introduction

The progress of such methods, as laser Doppler flowmetry [1–4], Doppler optical coherence tomography [5], intravital microscopy [6], magnetic resonance tomography and angiography [7], transcranial dopplerography [8], etc., allowed investigation of vascular system state and blood microcirculation in real time. Many of these methods suffer from essential limitations, such as insufficient spatial and temporal resolution, the limited information about the flow of particles, especially for in-depth scanning of biotissue, some invasiveness of measurements, etc. At present the most efficient diagnostic methods to determine the main parameters of microcirculation are those based on the dynamical scattering of light (laser Doppler flowmetry, LDF) [1–4], diffusion-wave spectroscopy [9, 10], speckle-visualisation [11–15], and the methods of computer biomicroscopy [6, 14, 16].

Note that in the modern medicine, when studying the blood circulation system, the issues related to the study of mechanisms of microcirculation of blood in norm and pathology are the key ones [17, 18], since it is just microcirculation that provides the delivery of oxygen and other necessary substances to individual organs and tissues, as well as the removal of metabolic products.

In the present work the study of capillary blood flow dynamics is carried out using the method of full-field speckle-correlometry [11–15], since it is a noninvasive contactless method that allows visualisation of capillary blood flow in real time without scanning of the laser beam. Full-field speckle-correlometry solves the problem of microcirculation imaging by means of the analysis of spatial statistics of time-averaged speckles, in particular, the analysis of spatial contrast of the speckle pattern. The method allows investigation of time-dependent scattering objects with complex dynamics, since it possesses greater temporal resolution as compared with the method of analysis of speckle pattern temporal contrast, where the values of contrast are calculated using a set of successively obtained images.

Important changes that allow more efficient monitoring of cerebral blood flow were introduced into the classical scheme [12–15], implementing the method of full-field speckle-correlometry. Thus, for visualisation of capillaries a microscope objective was used instead of a 'traditional' photo objective, and the probing radiation was transferred to the observing site via a silica-polymer optical fibre. In the course of experiments with laboratory animals *in vivo* one often meets with situations that make the measurements hard to perform. They include reflectory motions of the animal, the variation of biotissue optical parameters, e.g., due to oedema, etc. To provide partial compensation for the arising noise, an algorithm for automated tuning of the digital camera parameters was developed and incorporated in the program of contrast analysis.

In this paper we present the results of cerebral blood flow studies in laboratory rats under the conditions of developing stress-provoked stroke and administration of vasodilating and vasoconstrictive agents.

2. Materials and methods

2.1. Method of stroke modelling

We used the method of modelling stroke using stress [19], when a haemorrhage followed by blood microcirculation disturbance in the brain cortex occurs in the experimental animal. To control the changes in the blood flow velocity in all animals vasodilating and vasoconstrictive agents were administered intravenously using a catheter.

2.2. Method of measurements

The full-field speckle-correlometry – a simple and high-efficiency method used for blood flow imaging – was proposed in

M.A. Vilensky, O.V. Semyachkina-Glushkovskaya, P.A. Timoshina, Ya.V. Kuznetsova, I.A. Semyachkin-Glushkovskii, D.N. Agafonov
N.G. Chernyshevsky Saratov State University (National Research University), ul. Astrakhanskaya 83, 410012 Saratov, Russia;
V.V. Tuchin N.G. Chernyshevsky Saratov State University (National Research University), ul. Astrakhanskaya 83, 410012 Saratov, Russia; Institute for Problems of Precise Mechanics and Control, Russian Academy of Sciences, Rabochaya ul. 24, 410028 Saratov, Russia; University of Oulu, P.O. Box 4500, FIN-90014, Oulu, Finland;
e-mail: tuchinvv@mail.ru

Received 23 April 2012
Kvantovaya Elektronika **42** (6) 489–494 (2012)
Translated by V.L. Derbov

the middle of 1990s and is known as LASCA (LAser Speckle Contrast Analysis). It is based on closeness of statistical moments, describing spatiotemporal intensity fluctuations in ergodically and statistically homogeneous speckle fields, evaluated by means of averaging in time and space [12–15, 20–27].

With the aim of monitoring microhaemodynamics, the laboratory version of a full-field speckle-correlometer was developed, the scheme of which is presented in Fig. 1. The present setup allowed recording images of the same fragment of the sample both in coherent light (illumination by a laser) and in incoherent one (illumination by a light-emitting diode) without mechanical rearrangement. Since the final object of investigations is the blood flow, the speckle-imaging was implemented using the single-mode helium-neon laser GN-5P with the wavelength 633 nm, at which a substantial scattering of the probing radiation by red blood cells occurs. For microscopic studies we designed and used the ring illuminator, consisting of 12 light-emitting diodes with the central wavelength ~530 nm (AllLight, Guangdong, China). The choice of light emitting diodes was motivated by the fact that blood strongly absorbs light in the appropriate spectral region, which provides increased image contrast of the blood vessels. The laser beam was directed to the observing site through the silica-polymer optical fibre having the diameter 400 μm. Speckle-modulated images of the analysed surface area were recorded by means of the monochrome CMOS camera (Baslera802f, number of pixels in the matrix 656×491, pixel size 9.9×9.9 μm, 8 bit pixel^{-1}), equipped with the LOMO objective with the magnification 10$^{\times}$.

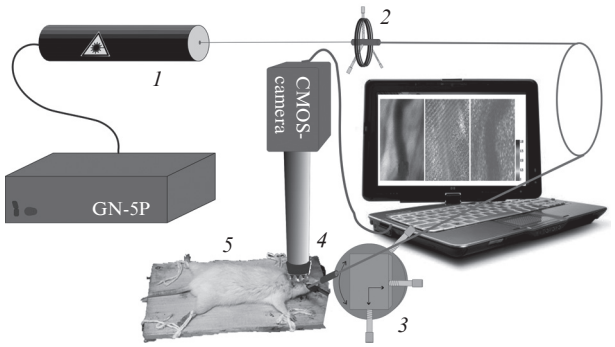

Figure 1. Schematic diagram of experimental setup: (*1*) He–Ne laser GN-5P with the wavelength 633 nm; (*2*) optical fibre; (*3*) detector (CMOS-camera Basler Z602f) (in the speckle-imaging regime); (*4*) lens tube of the microscope with microscopic objective (LOMO 10$^{\times}$) and 8-element light-emitting-diode illuminator (central wavelength ~530 nm); (*5*) object of study (in the microscopy regime).

In the full-field speckle-correlometry method the contrast of the dynamical time-averaged speckles is evaluated depending on the time of averaging of speckle-modulated images. To perform the measurements in real time it is necessary to average speckle-images during the time from 5 to 30 ms (in the experiments, described in the present paper, the exposure time of the CMOS camera was 20 ms). The rate of contrast reduction in the recorded speckles with increasing time of averaging depends on the mean time during which the moving scattering centres in the probed volume shift by the distance, equal to the wavelength of the probing radiation in the medium, and on the mean number of scattering events during the propagation of the radiation in the probed volume. The analysis of local contrast values of speckle-modulated images of the object surface at fixed exposure time over zones, including a given number of speckles, allows visualisation of regions, where the values of movability characteristics of scattering centres essentially differ from those, averaged over the entire probed area. During the processing of the speckle-modulated images of the analysed fragment of the biotissue surface, the values of contrast are calculated using the formula $V_k = \sigma_{I_k}/\bar{I}_k$, where k is the frame number in the sequence of speckle-modulated images;

$$\bar{I}_k = \frac{1}{MN}\sum_{m=1}^{M}\sum_{n=1}^{N} I_k(m,n)$$

is the brightness value, averaged over the analysed frame;

$$\sigma_{I_k} = \sqrt{\frac{1}{MN}\sum_{m=1}^{M}\sum_{n=1}^{N}[I_k(m,n) - \bar{I}_k]^2}$$

is the root-mean-square fluctuation component of the pixel brightness; M and N are the numbers of pixels in rows and columns of the analysed fragment of the frame, respectively; $I_k(m,n)$ is the pixel brightness in the kth frame.

Time averaging of the image of moving objects leads to reduced contrast for any type of the speckle motion. For random distribution of velocities the intensity of each speckle is fluctuating. In each individual case the problem of quantitative measurements is associated with understanding the interconnection between the contrast of speckles and the velocity of motion scattering centres (or velocity distribution) [22–26].

The relation between the velocity and the contrast is described as follows: the higher the velocity, the faster the fluctuations and the lower the contrast for the fixed exposure time. The interrelation between the contrast and the temporal autocorrelation function of intensity fluctuations is described by the expression [13, 15]:

$$\sigma_s^2(T) = \frac{1}{T}\int_0^T \tilde{g}_2(\tau)\,\mathrm{d}\tau, \qquad (1)$$

where σ_s^2 is the variance of the spatial intensity fluctuations in the speckle pattern; T is the exposure time; $\tilde{g}_2(\tau)$ is the covariance function of temporal intensity fluctuations of an individual speckle, which is an analogue of the autocorrelation coefficient:

$$\tilde{g}_2(\tau) = \frac{\bar{G}_2(\tau)}{\bar{G}_2(0)};\ \bar{G}_2(\tau) = \langle[I(t) - \langle I\rangle_t][I(t+\tau) - \langle I\rangle_t]\rangle_t. \qquad (2)$$

This relation determines the interrelation between the full-field speckle-correlometry and the methods that use intensity fluctuations of the laser light, scattered by a moving object or particle. Full-field speckle-correlometry uses speckle-modulation in the zone of the image, while the basic temporary methods use speckle-modulation in the far-field zone.

In principle, all these methods allow determination of the correlation time τ_c. In the case of full-field speckle-correlometry some additional assumptions should be made to specify the relation between the measured speckle contrast (defined as $\sigma_s/\langle I\rangle$) and the correlation time τ_c. Depending on the type of the studied motion, different models may be used. For the Lorentz velocity distribution the equation takes the form [13, 15]

$$\frac{\sigma_s}{\langle I\rangle} = \left\{\frac{\tau_c}{2T}\left[1 - \exp\left(-\frac{2T}{\tau_c}\right)\right]\right\}^{1/2}. \qquad (3)$$

This equation relates the speckle contrast, calculated as the ratio of the root-mean-square intensity fluctuation to the mean intensity, and the correlation time τ_c for given T.

From this point of view the full-field speckle-correlometry meets the same problems as all frequency-temporal methods, namely, the evaluation of the correlation time is affected by the form of the velocity distribution of scattering particles, multiple scattering, size of the particles (in the present case, red blood cells), shape of scatterers, non-Newtonian flow of the liquid, non-Gaussian statistics due to small number of scatterers, etc. Due to uncertainties caused by the mentioned factors, one should rely on appropriate calibration using dynamic phantoms of biotissues rather than on absolute measurements, when using these methods.

To measure the temporal statistics of a fluctuation speckle pattern one has to trace the intensity of an individual speckle. In this case the detector aperture must be smaller than the mean speckle size, otherwise a certain spatial averaging appears and the first-order statistics is disturbed. The full-field speckle-correlometry implies calculation of the local contrast of speckles using a set of pixels, the number of which is controlled by the operator. The wider the processed area, the better the statistics. But it is also important to process a large enough number of speckles, not only of pixels; if the speckles are much larger than the pixels, then a smaller number of speckles are processed. This circumstance means that the suitable size of speckles is limited. If the speckles are too small, then each pixel contains more than one speckle, which leads to their averaging and reduces the measured contrast. If the speckles are large, then the present number of speckles can appear insufficient to provide good-quality statistics. Therefore, the size of speckles should be carefully controlled, which can be implemented by choosing the aperture of the optical system, forming the image, because only it determines the speckle size. On the other hand, this can limit the possibility to control the light flux entering the camera, since the camera shutter exposure time is specified by the range of the velocities measured. If the dynamic range of the camera is not very large, this may become a serious limitation and require using neutral filters to provide the level of the light flux acceptable for the detector.

Another problem is the impossibility to obtain experimentally the whole range of contrast variation, described by theory. A stationary object must give the contrast equal to unity ($\sigma = \langle I \rangle$). A completely smeared speckle pattern, arising in the case of fast motion of scatterers, must have zero contrast. For example, the Lorentz model predicts the dependence of the contrast $\sigma/\langle I \rangle$ on τ_c/T. For the given exposure time T the dynamic range of the contrast measurement from 0.1 to 0.9 must correspond to nearly 2.5 orders of magnitude for τ_c (and, therefore, the velocity).

Practically, even for stationary random scatterers the measured contrast is equal to 0.6 [12]. One of the reasons is the CCD camera itself. Most of the CCD cameras are designed to have a shift of the constant component with respect to zero, called a pedestal. This is done to prevent cutting of negative peaks, arising in the course of processing. The pedestal gives rise to a shift of the probability density histogram along the x axis with corresponding influence on the root-mean-square value and, therefore, on the contrast. By the appropriate data processing one can eliminate the influence of dark current. Then the measured contrast of the image of a stationary diffuse surface increases from 0.41 to 0.95, which is close to the theoretical value, equal to one for fully developed speckles [13]. Under the same conditions the contrast of the speckle pattern, obtained from a fragment of human skin, increases from 0.33 to 0.68. The smaller contrast, as compared with the case of stationary scatterers, is due to the effect of moving scatterers (red blood cells) in the tissue volume. Other statistical problems are associated with the Gaussian profile of the laser beam and with the nonlinearity of the CCD camera [13].

To perform the measurements and to calculate the contrast we developed a program in the LabVIEW 8.5 environment (National Instruments, USA) that allows real-time recording of the intensity distribution of the speckle field with the rate of 100 frames per second and calculation of the mean contrast or its spatial distribution using Eqn (1) with parallel visualisation in the region chosen by the operator. The block diagram of calculating the contrast and the distribution of the contrast local estimates is presented in Fig. 2. Figure 3 shows the images

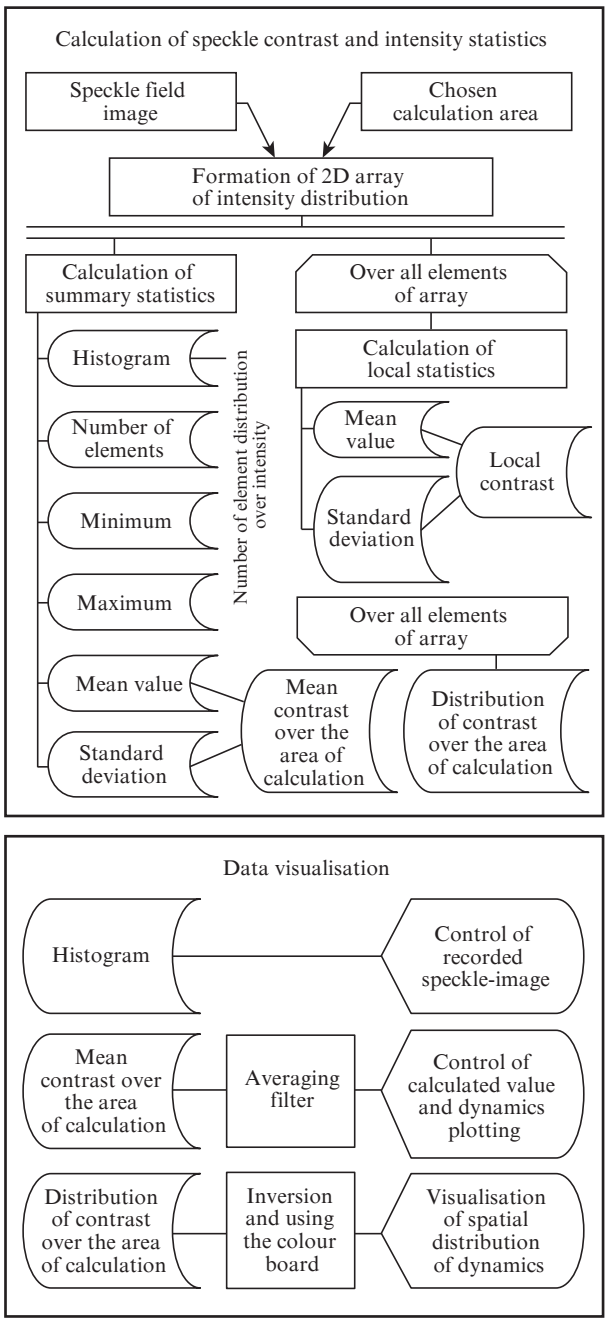

Figure 2. Block diagram of calculation of contrast and intensity distribution in speckle patterns.

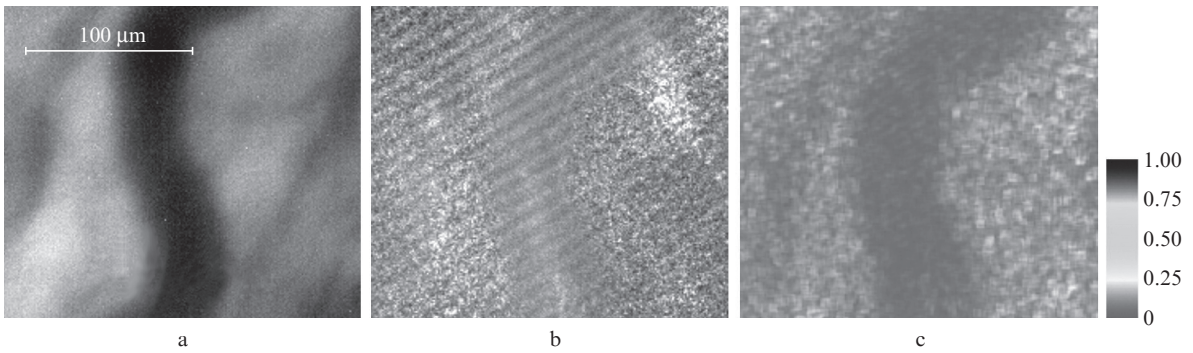

Figure 3. Microscopic image of a typical blood vessel (a), spatial distribution of local contrast estimates (b), and spatial distribution of the local estimates of contrast after normalisation in the zone of the vessel (c).

of a typical blood vessel, obtained by means of the method of digital microscopy, the method of spatial distribution of local contrast estimates, and after normalisation of this distribution. One of the most important parameters in the studies of the contrast is the time of speckle pattern recording, i.e., the exposure time. In spite of the possibility (in certain limits) to exercise programmed control of the camera exposure, in the real experiment there are limitations that do not allow choosing any available exposure. Thus, in connection with different absorption and scattering coefficients in different samples, and with the difference in their internal dynamics (or in case of significant temporary and spatial variations of these parameters within a single sample) at constant intensity of the incident radiation one can observe essential difference in the statistics of the recorded distribution of intensity fluctuations, and, therefore, in the contrast, calculated on its basis.

The algorithm of automated tuning of the digital camera parameters, which was developed and incorporated into the used program of the contrast analysis, allowed partial compensation of the abovementioned differences by means of the optimal choice of the amplification and brightness at fixed exposure. Nevertheless, in the cases of insufficient acquisition time or excess light, incident on the light-sensitive elements of the camera during the exposure time, the statistics of the intensity fluctuations in the recorded image is disturbed. This happens due to insufficient sensitivity or 'overload' of the light-sensitive elements of the detector.

3. Discussion of the results

The developed software allowed calculation of the contrast spatial distribution from the experimental data obtained in the study of the cerebral blood flow in animals (Table 1), and also successful investigation of the dynamics of blood microcirculation in the human nail bed under occlusion (not presented in this publication). The result of the program operation consists in calculating the spatial distribution of the contrast, obtained from five sequential images of the dynamical speckle pattern.

Table 1 presents the experimental values of the contrast, obtained as a result of speckle-correlation monitoring of blood microcirculation in the surface layers of the brain cortex of experimental animals in normal state and in the cases of artificially induced pathologies. The data summarised in the Table, corresponding to stabilised haemodynamic regimes in norm and pathologies, are the results of averaging over sets of experimentally measured contrast values in different experimental animals. In correspondence with the procedure of evaluating

Table 1. Dynamics of contrast under varying functional conditions of experimental animals.

Group of animals	Mean contrast value			
	Before administration of vasoconstrictive agent	After administration of vasoconstrictive agent	Before administration of vasodilating agent	After administration of vasodilating agent
1	0.30±0.02 0.33±0.01	0.14±0.01 0.27±0.01	0.31±0.01 0.31±0.01 0.32±0.01	0.36±0.02 0.34±0.01 0.36±0.01
2	0.24±0.01 0.33±0.01	0.15±0.01 0.25±0.01	0.27±0.01 0.33±0.01 0.20±0.01	0.32±0.03 0.37±0.02 0.32±0.02
3	0.26±0.01 0.28±0.01 0.24±0.01	0.21±0.01 0.23±0.01 0.22±0.01	0.27±0.01 0.24±0.01	0.40±0.02 0.31±0.02

the confidence interval Δ_ξ with the distribution function of the measured random variable ξ being unknown [28], the values of Δ_V were specified as $\Delta_V \approx 1.6\sigma$ for the significance level 0.9. The expected result is the increase of time-averaged speckles contrast due to suppression of microhaemodynamics by the intravenous injection of a vasodilating agent. On the contrary, the intravenous injection of a vasoconstrictive agent is expected to cause increased haemodynamic intensity and essential reduction of contrast as compared with the normal state.

The results of the studies have shown that in the stabilised physiological regime in healthy animals (the third group) the contrast, depending on the blood microcirculation, varies from 0.24 to 0.28. In 24 hours after the stress impact (the first group of animals) the velocity of capillary blood flow was reduced, which could be seen from the contrast of 0.3–0.33, increased as compared with the normal state. The reduction of the capillary blood flow intensity on the next day after the stroke, induced in the animals under study, is an expected result. The monitoring of the blood microcirculation state directly after the stress impact (the second group of animals) revealed changes in the contrast value with respect to the normal state only in two animals (the contrast increased up to 0.33). The change of the contrast, and, correspondingly, the state of blood microcirculation under the administration of vasodilating and vasoconstrictive agents was also in agreement with the expected physiological response (dilation and constriction of the blood vessels and appropriate changes of the blood flow velocity) to the action performed. Hence, the method of speckle-imaging allows real-time tracing of the changes in blood microcirculation state.

For the proposed method of full-field speckle-correlation monitoring using the multimode optical fibre to transport the laser radiation to the probed site the contrast does not exceed 0.6 even in the cases of probing steady-state multiply-scattering media (e.g., model scatterers based on polymer layers). One of the reasons that cause such low values of the contrast of detected speckle-modulated images is the depolarisation of laser radiation in the course of its propagation in multimode optical fibres. As a result, the speckle field, produced in the detection zone and being macroscopically depolarised, may be presented as a superposition of two statistically independent developed-speckle fields having mutually orthogonal directions of polarisation [29, 30]; in this case the maximal possible contrast for the resulting steady-state speckle field is equal to $\sim$0.7. Other factors that reduce the contrast are non-controllable microscopic vibrations of elements of the speckle-correlometry system (in the first place, the optical fibre), as well as instrumental errors in recording the dynamical speckle-modulated images by the CMOS array.

Significant variations of the contrast, caused by the changes in blood microcirculation, are observed in our experiments with the exposure time 20 ms; in this case the characteristic time of red blood cell displacement $\lambda/\bar{v}$ by the distance of the order of the probing radiation wavelength due to their motion in the microcirculatory bed amounts to 10^{-3}–10^{-2} s. On the other hand, preliminary studies of the possibility to calibrate the speckle-correlometry system using a flow of a scattering liquid (a suspension of polydisperse particles in water) with fixed velocity in a polystyrene tube having the diameter 3 mm have shown that at the exposure of 20 ms the values of $V(T)$, obtained by detecting the flow-scattered radiation, vary from 0.4 to 0.04 when the flow velocity varies from 30 to 400 μm s^{-1} [31].

One of the possible future applications of the full-field speckle-correlation method in the clinical practice is low-invasive monitoring of cerebral blood microcirculation in the brain of small animals without craniotomy under the conditions of immersion optical clearing of the skin and bone head tissues by means of hyperosmotic agents [32–34] and using alternative algorithms for speckle pattern processing [35–37]. For example, the authors of [36] reported the results of cerebral blood flow monitoring using the full-field speckle-correlation method with temporal averaging without damaging the brain-pan of a rat. Among the publications, devoted to the solution of this problem, paper [38] is worth mentioning, in which the efficiency of combined application of optical clearing technique and full-field speckle-correlometry to the monitoring of strongly scattering media with pronounces dynamics of scatterers is investigated. The recently published paper [39] reports a successful application of the full-field speckle-correlometry method to the monitoring of cerebral blood flow with the use of the optical clearing method.

Thus, the experimental study of the blood flow velocity dynamics under the conditions of stroke in laboratory rats demonstrates high efficiency of the developed instrument and algorithm for data acquisition and processing, implementing the method of full-field speckle-imaging, in monitoring of the blood microcirculation state in the brain cortex, affected by pathological changes or action of agents.

Acknowledgements. The authors express particular gratitude to V.A. Berdnikova, Associate Professor of the Chair of Physiology of Plants and Animals, Department of Biology, Saratov State University, for the help in preparation of laboratory animals.

The dynamical biotissue phantom was offered by the Research-Educational Institute of Optics and Biophotonics, Saratov State University. The authors are particularly grateful to developers V.V. Lychagov, E.A. Genina, A.N. Bashkatov, and V.I. Kochubey.

The work was carried out in the framework of State Contract No. 02.740.11.0879 and was supported by the Grant of the RF President (Grant No. NSh-1177.2012.2 for Support of Scientific Schools), by the Ministry of Education and Science of Russia (Research Grant No. 0121158566), by the European Commission (7th Frame Programme – Photonics4Life, Grant No. 224014), and by the Program FiDiPro TEKES (40111/11), Finland.

References

1. Bonner R., Nossal R. *Appl. Opt*., **20**, 2097 (1981).
2. Serov A., Steinacher B., Lasser T. *Opt. Express*, **13**, 3681 (2005).
3. Dunn A.K., Bolay H., Moskowitz M.A., Boas D.A. *J. Cereb. Blood Flow Metab*., **21**, 195 (2001).
4. Peiponen K.-E., Myllylä R., Priezzhev A.V. *Optical Measurement Techniques, Innovations for Industry and the Life Science* (Berlin – Heidelberg: Springer-Verlag, 2009).
5. Tuchin V.V. (Ed.) *Coherent-Domain Optical Methods: Biomedical Diagnostics, Environmental and Material Science* (Boston: Kluwer Acad. Publ., 2004) Vols 1 & 2.
6. Kalchenko V., Harmelin A., Fine I., Zharov V., Galanzha E., Tuchin V. *Proc. SPIE Int. Soc. Opt. Eng.*, **6436**, 64360D-1-15 (2007).
7. Bryan R.N., Levy L.M., Whitlow W.D., Killian J.M., Preziosi T.J., Rosario J.A. *Am. J. Neuroradiol.*, **12**, 611 (1991).
8. Razumovsky A.Y., Gillard J.H., Bryan R.N., Hanley D.F. *Acta Neurol. Scand*., **99**, 65 (1999).
9. Zimnyakov D.A. *Coherent-Domain Optical Methods: Biomedical Diagnostics, Environmental and Material Science*. Ed. by V.V. Tuchin (Boston: Kluwer Acad. Publ., 2004) Vol. 1, pp 3–41.
10. Meglinskii I.V., Tuchin V.V. *Coherent-Domain Optical Methods: Biomedical Diagnostics, Environmental and Material Science*. Ed. by V.V. Tuchin (Boston: Kluwer Acad. Publ., 2004) Vol. 1, pp 139–164.
11. Vilenskii M.A., Agafonov D.N., Zimnyakov D.A., Tuchin V.V., Zdrazhevskii R.A. *Kvantovaya Elektron.*, **41** (4), 324 (2011) [*Quantum Electron*., **41** (4), 324 (2011)].
12. Briers J.D., Webster S. *J. Biomed. Opt*., **1**, 174 (1996).
13. Briers J.D. *Physiol. Meas*., **22**, 35 (2001).
14. *Advanced Optical Flow Cytometry: Methods and Disease Diagnoses*. Ed. by V.V. Tuchin (Weinheim: Wiley-VCH Verlag GmbH & Co. KGaA, 2011).
15. Zimnyakov D.A., Briers J.D., Tuchin V.V., in *Handbook of Optical Biomedical Diagnostics*. Ed. by V.V. Tuchin (Bellingham: SPIE Press, 2002) pp 987–1036.
16. Galanzha E.I., Brill G.E., Aizu Y., Ulyanov S.S., Tuchin V.V., in *Handbook of Optical Biomedical Diagnostics*. Ed. by V.V. Tuchin (Bellingham: SPIE Press, 2002) pp 881–938.
17. Pokrovskii A.V., Kiyashko V.A. *Russkii Meditsinskii Zhurnal*, No. 12, 691 (2011).
18. Fedin A.I., Ermoshkina N.Yu., Soldatov M.A. *Nevrologicheskii Zhurnal*, **12** (2), 18 (2007).
19. Romanova T.P. *Patologicheskaya Fiziologiya i Eksperimental'naya Terapiya*, **3**, 80 (1989).
20. Zimnyakov D.A., Agafonov D.N., Sviridov A.P., Omel'chenko A.I., Kuznetsova L.V., Bagratashvili V.N. *Appl. Opt.*, **41** (28), 5984 (2002).
21. Zimnyakov D.A., Sviridov A.P., Kuznetsova L.V., Baranov S.A., Ignat'eva N.Yu., Lunin V.V. *Zh. Fiz. Khim.*, **81** (4), 725 (2007) [*Russian J. Phys. Chem*., **81** (4), 626 (2007)].
22. Boas D.A., Dunn A.K. *J. Biomed Opt*., **15** (1), 011109 (2010).
23. Yuan S., Devor A., Boas D.A., Dunn A.K. *Appl. Opt*., **44**, 823 (2005).
24. Wang Z., Luo Q.M., Cheng H.Y., Luo W.H., Gong H., Lu Q. *Prog. Nat. Sci*., **13**, 522 (2003).
25. Zakharov P., Bhat S., Schurtenberger P., Scheffold F. *Appl. Opt*., **45**, 1756 (2006).

26. Jiang C., Zhang H., Wang J., Wang Y., He H., Liu R., Zhou F., Deng J., Li P., Luo Q. *J. Biomed. Opt*., **16** (11), 116008 (2011).
27. Ulianova O.V., Ulianov S.S., Li P., Luo C. *Kvantovaya Elektron.*, **41** (4), 340 (2011) [*Quantum Electron*., **41** (4), 340 (2011)].
28. Novitskii P.V., Zograf I.A. *Otsenka pogreshonstei rezul'tatov izmerenii* (Evaluation of Measurement Errors) (Leningrad: Energoatomizdat, 1985).
29. Serov A., Steenbergen W., de Mul F. *J. Opt. Soc. Am. A*, **18**, 622 (2001).
30. Goodman J. *Statistical Optics* (New York: Wiley, 1985).
31. Zimnyakov D.A., Tuchin V.V., Yodh A.G. *J. Biomed. Opt*., **4** (1), 157 (1999).
32. Agafonov D.N., Timoshina P.A., Vilenskii M.A., Fedosov I.V., Tuchin V.V. *Izv. SGU., Ser. Fiz.*, **11** (2), 14 (2011).
33. Bashkatov A.N., Genina E.A., Sinichkin Yu.P., Kochubey V.I., Lakodina N.A., Tuchin V.V. *Biophys. J*., **85** (5), 3310 (2003).
34. Genina E.A., Bashkatov A.N., Tuchin V.V. Doi:10.1155/2008/267867.
35. Bashkatov A.N., Genina E.A., Tuchin V.V. *Handbook of Biomedical Optics*. Ed. by D.A. Boas, C. Pitris, N. Ramanujam (London: Taylor & Francis Group, CRC Press Inc., 2011) Ch. 5.
36. Ayata C., Shin H.K., Salomone S., Ozdemir-Gursoy Y., Boas D.A., Dunn A.K., Moskowitz M.A. *J. Cereb. Blood Flow Metab*., **24**, 1172 (2004).
37. Li P., Ni S., Zhang L., Zeng S., Luo Q. *Opt. Lett*., **31** (12), 1824 (2006).
38. Wang J., Zhu D., Chen M., Liu X. *Innov. J. Opt. Health Sci*., **3** (3), 159 (2010).
39. Wang J., Zhang Y., Xu T., Luo Q., Zhu D. *Laser Phys. Lett*., **9** (6), 469 (2012).